The Ochsner Journal 13:76–90, 2013

Nelfinavir Suppresses Insulin Signaling and Nitric Oxide Production by Human Aortic Endothelial Cells: Protective Effects of Thiazolidinediones

Debasis Mondal, PhD,* Kai Liu, PhD,* Milton Hamblin, PhD,* Joseph A. Lasky, MD,† Krishna C. Agrawal, PhD*[1]

**Department of Pharmacology and*
†Section of Pulmonary Diseases, Tulane University Medical Center, New Orleans, LA

ABSTRACT

Background: In human immunodeficiency virus 1 (HIV-1)–infected individuals, exposure to a protease inhibitor (PI)-based highly active antiretroviral therapy (HAART) regimen increases cardiovascular disease and endothelial dysfunction. However, the mechanisms of PI-induced effects on endothelial cells (ECs) are not known. Furthermore, strategies to suppress these deleterious outcomes of PIs need to be developed. Insulin-induced PI3K/Akt signaling and endothelial nitric oxide (NO)-synthase (eNOS) phosphorylation regulates NO production by ECs that maintain vascular homeostasis. We evaluated whether nelfinavir (NEL), a potent HIV-1 PI that suppresses Akt phosphorylation, can alter insulin-induced NO production in human aortic endothelial cells (HAECs) and whether insulin sensitization of HAECs via the peroxisome proliferator-activated receptor-gamma agonists, thiazolidinediones, can ameliorate these side effects.

Methods: Real-time NO production in HAECs was monitored by fluorimetric dyes DAF-FM DA and DAF-2 DA. Immunodetection studies were used to determine the phosphorylation of Akt, eNOS, insulin receptor-β (IR-β), insulin receptor substrate-1 (IRS-1), and PI3K/p85α. Expression of eNOS messenger RNA was measured by reverse transcription polymerase chain reaction.

Results: In vitro exposure (72 hours) of HAECs to NEL (0.25-2 μg/mL) decreased both basal (2.5-fold) and insulin-induced NO production (4- to 5-fold). NEL suppressed insulin-induced phosphorylation of both Akt and eNOS at serine residues 473 and 1177, respectively. NEL decreased tyrosine phosphorylation of IR-β, IRS-1, and PI3K. Coexposure to troglitazone (TRO; 250 nM) ameliorated the suppressive effects of NEL on insulin signaling and NO production. Coexposure to TRO also increased eNOS expression in NEL-treated HAECs.

Conclusion: Our findings indicate that treatment with potent insulin sensitizers may protect against PI-mediated endothelial dysfunction during long-term HAART.

Address correspondence to
Debasis Mondal, PhD
Associate Professor
Department of Pharmacology, SL 83
Tulane University Health Sciences Center
1430 Tulane Ave.
New Orleans, LA 70112-2699
Tel: (504) 988-4668
Fax: (504) 988-5283
Email: dmondal@tulane.edu

Keywords: Endothelial cells, HIV-1, nelfinavir, nitric oxide, thiazolidinediones

Funding: This study was supported in part by grants from the Louisiana Cancer Research Consortium (DM) and the National Institutes of Health: R01-HL63128 (KCA, DM), R01-HL073691 (KCA, DM), and R01- HL083480 (JL, DM).

[1]This work was carried out in collaboration with Prof. Krishna C. Agrawal (past chairman of the Department of Pharmacology at Tulane University) and his postdoctoral fellow Dr Kai Liu. In a tragic accident on December 11, 2009, Dr Agrawal passed away. May God rest his soul. Afterward, Dr Liu returned to China. The work has been recently completed by Dr Debasis Mondal and Dr Milton Hamblin and is dedicated to the memory of Dr Agrawal.

INTRODUCTION

The advent of human immunodeficiency virus 1 (HIV-1) protease inhibitors (PIs) and their combination with HIV-1 reverse transcriptase inhibitors (RTIs) revolutionized the treatment against AIDS.[1] This highly active antiretroviral therapy (HAART) regimen has significantly decreased morbidity and mortality in HIV-1 positive patients.[2,3] However, severe side effects associated with chronic HAART dampened the initial enthusiasm.[4] Although similar side effects were described in HIV-positive patients receiving only RTIs, their frequency and severity were significantly greater in patients on chronic PI-based HAART.[5-7]

Cardiovascular problems—including cardiomyopathy, pulmonary hypertension, arrhythmias, endocarditis, coronary artery disease, and atherosclerosis—were reported in these individuals. In addition, increased incidence of lipodystrophy, dyslipidemia, and visceral adiposity raised concerns related to diabetes and accelerated atherosclerosis. These changes in body habitus, collectively known as metabolic syndrome, were believed to be manifested via the induction of an insulin resistance syndrome that indicated impaired action of insulin in both vascular endothelial cells (ECs) and adipocytes.

Severe side effects were observed with first generation PIs—such as indinavir, ritonavir, saquinavir, and nelfinavir (NEL)—and although less severe, cardiovascular side effects are also being documented with newer PIs like lopinavir, amprenavir, and atazanavir.[8-10] In this study, we focused on the mechanism of action of NEL, primarily because this drug has shown the highest level of metabolic side effects[11,12] and secondly because NEL is currently being tested in several clinical trials as an anticancer agent[13,14] where its deleterious effects may also be manifested.

Vascular ECs are chronically exposed to high plasma concentrations of PIs; therefore, the observed side effects may be a direct consequence of endothelial dysfunction.[15,16] However, although a number of previous studies investigated the molecular mechanisms of PI-induced lipid abnormalities and possible treatment options,[17-19] comparatively little is known about PI effects on vascular ECs, and strategies to suppress PI-induced cardiovascular effects are lacking.[20-22]

Although data strongly suggest that PIs negatively impact the vasculature[15,22] and although endothelial dysfunction is a predictor of cardiac events,[23,24] molecular mechanisms linked to NEL-induced effects on ECs are not known. Changes in vascular homeostasis are a well-established response to cardiovascular risk factors and are early markers of atherosclerosis.[25,26] Multiple metabolic and clinical predictors of endothelial dysfunction and evidence of carotid intima-media thickness were observed in HIV-infected subjects.[27] Schillaci et al[28] demonstrated that HIV-infected patients under PI-based HAART had higher values of aortic stiffness. Simultaneous ultrasound and applanation tonometry of the common carotid artery showed that endothelial nitric oxide (NO) synthase (eNOS) inhibition increases carotid stiffness in humans.[29] Furthermore, recent studies demonstrate increased intima-media thickness and alterations in the structural characteristics of epiaortic lesions in patients receiving PIs.[30] Therefore, we carried out in vitro investigations of NEL-induced molecular dysfunction on primary human aortic endothelial cells (HAECs).

A principal mediator of normal endothelial function is the endothelium-derived relaxing factor (EDRF) NO that regulates vessel homeostasis by inhibiting vascular smooth muscle contraction and growth, platelet aggregation, and leukocyte adhesion to the endothelium.[31] In normal ECs, the enzyme eNOS converts L-arginine to L-citrulline and NO that signal the surrounding smooth muscle to relax, thus resulting in vasodilation and increased blood flow. Therefore, there is a close relationship between insulin-mediated glucose disposal and the incremental increase in blood flow in response to insulin. However, this normal response is lost in insulin-resistant states, resulting in the impairment of NO synthesis and in endothelial dysfunction.[32] In addition to inhibiting NO production, impairment of the cellular redox system may also contribute to endothelial dysfunction.[33] Previous studies[34-36] have indicated that several PIs can induce vascular dysfunction via the induction of oxidative stress. The role of chronic oxidative stress in vascular injury and dysregulation of the eNOS system in ECs is also well known, and studies show that the expression of eNOS can be decreased in both porcine and human pulmonary arteries treated with different HIV-1 PIs.[37] However, it is not known whether these PIs directly suppress the insulin signaling cascade.

Insulin-induced second messenger signaling results in eNOS phosphorylation and activation via the tyrosine kinase-activity present in the insulin receptor substrate-1 (IRS-1). Indeed, IRS-1 is known to be the major substrate activated following insulin binding to its receptor (IR).[38] Insulin stimulation activates receptor kinase functions, resulting in stimulation of insulin receptor beta (IR-β) and then IRS-1. The PI3K/Akt signaling pathway also plays a central role in controlling vascular function, and insulin regulates endothelial biology by activating Akt phosphorylation, which then stimulates endothelial NO production.[39] Defective PI3K/Akt signaling in endothelial cells can lead to the development of insulin resistance in type 2 diabetic models. The Akt protein is a serine/threonine kinase that is activated via the tyrosine kinase receptor of IR-β. Tyrosine phosphorylation of IR-β provides binding sites for specific Src homology (SH2) domain proteins including the 85 kDa regulatory subunit of phosphatidylinositol 3-kinase (PI3K/p85α), which then activates the p110 catalytic subunit of PI3K/Akt. Because NEL exposure has been shown to suppress Akt phosphorylation in different cell types,[40] we investigated whether NEL exposure can suppress insulin signaling, Akt and eNOS phosphorylation, and NO production in HAECs. In

addition, we monitored whether insulin sensitization of these cells can overcome the suppressive effects of NEL.[41]

Thiazolidinediones (TZDs), commonly used as antidiabetic agents and vasoprotective compounds, act as potent insulin sensitizers because of their agonistic activity on the nuclear transcription factor, peroxisome proliferator-activated receptor-gamma (PPAR-γ).[42] Numerous studies have shown that PPAR-γ can directly enhance Akt phosphorylation in insulin-sensitive tissues such as endothelial cells, smooth muscle cells, and adipocytes. Studies focusing on the vasculature have revealed complex relationships between PPAR-γ and PI3K/Akt signaling pathways; recent reports suggest that PPAR-γ could be a target of Akt.[38,39,41] In endothelial cells, prolonged treatment with TZDs increased NO production via Akt-mediated phosphorylation of eNOS. It has also been reported that TZDs, beyond their ability to improve glycemic control, can regulate and normalize endothelial and vascular smooth muscle cell function, as well as mitigate inflammatory responses in vessel walls.[43] Apart from improving tissue insulin sensitivity and lowering blood glucose, several clinically approved TZDs—such as troglitazone (TRO), rosiglitazone, ciglitazone, and pioglitazone—are also known to exert beneficial effects on the cardiovascular system. Although TRO was one of the most potent TZDs approved for the treatment of type 2 diabetes, it had to be withdrawn because of severe drug-induced liver injury.[44] We used TRO as a proof-of-principle agent to examine whether a potent TZD can suppress NEL-induced dysfunctions in HAECs.

METHODS

Reagents

NEL tablets were obtained from the Tulane University Clinic (New Orleans, LA). These tablets (Viracept) were pulverized in a mortar and dissolved in anhydrous ethanol at a 10 mg/mL concentration. TRO powder was purchased from Alexis Corporation (Lausen, Switzerland) and dissolved in dimethyl sulfoxide at a 10 mM stock solution. Both drugs were filtered (0.2 μm), stored in aliquots at –20°C, and diluted in culture medium before being added to the cells. Insulin solution (10 mg/mL) was obtained from Sigma-Aldrich (Saint Louis, MO) and stored in aliquots at –4°C. The fluorescent dyes used for real-time quantitation and bioimaging of NO, 4-amino-5-methylamino-2′,7′-difluorofluorescein diacetate (DAF-FM DA) and 4,5-diaminofluorescein diacetate (DAF-2 DA), respectively, were purchased from Calbiochem (La Jolla, CA). Antibodies to PI3K/Akt (against both nonphosphorylated and phosphorylated [serine residue {Ser}473] Akt) were obtained from Cell Signaling (Beverly, MA). Antibodies to eNOS (against both nonphosphorylated and phosphorylated [Ser1177] eNOS proteins) were obtained from BD Biosciences (San Jose, CA). Antibodies to IR-β (against both nonphosphorylated and phosphorylated IR-β proteins) were purchased from Santa Cruz Biotechnology (Santa Cruz, CA). Antibodies to nonphosphorylated IRS-1 and PI3K/p85α and the antibody to phosphorylated tyrosine residues were purchased from Upstate Biotechnology (Lake Placid, NY). Antibodies to β-actin, goat antirabbit immunoglobulin (IgG), and horseradish peroxidase (HRP)-conjugated rabbit antimouse IgG were purchased from Sigma-Aldrich.

Cell Culture

Primary HAECs were obtained from Clonetics/Bio-Whittaker Inc. (San Diego, CA).[34] Cells were maintained in endothelial cell growth medium-2 (Cambrex Bio-Science Walkersville, Inc., Walkersville, MD) containing endothelial cell basal medium-2, hydrocortisone, basic fibroblast growth factor, vascular endothelial growth factor, insulin-like growth factor-1, ascorbic acid, epidermal growth factor, heparin, and 2% fetal bovine serum. Cells obtained as passage 3 were cultured in T-75 flasks at 37°C in a humidified incubator with 5% CO_2 atmosphere. Cells were passaged every week and subcultured at a ratio of 1:3. The medium was changed twice weekly and all cultures were used within 3 weeks; all experiments were conducted within 3-5 more passages. Cells were regularly verified as endothelial cells by checking their ability to produce factor VIII-related antigen by immunofluorescence microscopy.

Treatments

For chronic exposure experiments, cells were treated with NEL and/or TRO for 72 hours and drugs were replenished every 24 hours. HAECs were cultured to 70%-80% confluency and then exposed to NEL for 72 hours, followed by insulin stimulation for 10 minutes. Cells were then harvested and fixed for microscopy, or protein extracts were obtained for immunoblotting. Both quantitation and bioimaging of NO were carried out by using fluorimetric assays. The phosphorylation of proteins involved in the insulin signaling cascade was monitored by Western blot. For insulin-induced eNOS gene expression, total RNA was harvested from cells treated for 72 hours with NEL and with or without insulin stimulation for the last 8 hours. In all experiments, control cultures were exposed to the proper vehicle consisting of the drug diluents only.

NO Measurements

DAF-2 DA was used for fluorescence microscopy of NO,[45] and real-time measurements of NO production by fluorimetry were carried out using DAF-FM DA.[46] For microscopy studies, HAECs were cultured on coverslips in 6-well plates and treated for the indicated times with different drug concentrations. Cells were washed and phenol red-free media was added, and then cells were incubated with DAF-2 DA (5 μM) for 10 minutes in the dark. Cells were then washed twice with ice-cold phosphate-buffered saline (PBS), fixed with 2% paraformaldehyde for 3 minutes and washed twice again with ice-cold PBS. Coverslips were then mounted onto slides with Gel Mount (Sigma-Aldrich), and analysis of NO production was carried out using a Nikon microscope (ECLIPSE 80*i*) with the excitation wavelength set at 480 ± 10 nm and the emission wavelength at 505 ± 10 nm. The images were captured by a SensiCam camera with IPLab 3.65a software (Scanalytics, Inc., Fairfax, VA). All images were taken during the first 30 seconds of light exposure to avoid fluorescence decay. DAF-FM DA is a pH-insensitive dye that reacts with NO to form the fluorescent product DAF-FM T. For fluorimetry experiments, HAECs were cultured in 24-well black plates (Labnet International, Woodbridge, NJ). After 72 hours, cells were washed twice with ice-cold PBS and incubated with DAF-FM DA (5 μM) at 37°C. Following incubation, cells were washed with ice-cold PBS and incubated at 37°C with L-arginine (100 μM) for 15 minutes. NO levels were determined by fluorescence readings (from bottom of plate) by using an *FL$_x$800* fluorimeter (BioTek Instruments, Winooski, VT) with the excitation and emission wavelengths set at 485 ± 10 nm and 525 ± 10 nm, respectively. No dye controls were used as background fluorescence and were subtracted from readings with all dye-containing sample wells. Subsequently, cells were lysed, proteins were quantified using the Pierce (Rockford, IL) BCA Protein Assay Kit, and NO levels were normalized to protein content.

Immunoblotting and Immunoprecipitation

For both immunoblotting and immunoprecipitation studies, cell lysates were obtained from HAECs grown in 100-mm culture dishes. After specified treatments, cells were washed with ice-cold PBS and lysed with 1× cell lysis buffer (Cell Signaling). The lysis buffer consisted of 20 mM Tris-HCl (pH 7.5), 150 mM NaCl, 1 mM Na_2EDTA, 1 mM EGTA, 1% Triton, 2.5 mM sodium pyrophosphate, 1 mM β-glycerophosphate, 1 mM Na_3VO_4, 1 μg/mL leupeptin, and 1 mM PMSF. Furthermore, the PI and phosphatase inhibitor cocktails from Sigma-Aldrich were added to the lysis buffer (1:100 dilution) immediately before use. Cell debris was removed by centrifugation at 13,000 × g for 15 minutes, protein concentrations were measured with the BCA kit, and aliquots were used in the immunoblot and immunoprecipitation experiments as stated below. For immunoblot studies, approximately 50 μg of protein samples was electrophoresed on a 7.5% sodium dodecyl sulfate-polyacrylamide gel electrophoresis (SDS-PAGE) gel and transferred to a nitrocellulose membrane (BIO-RAD, Hercules, CA) using a semi-dry transfer apparatus (BIO-RAD) at 20 volts for 45-60 minutes. After incubation with blocking buffer for 1 hour at room temperature, the membranes were washed 3 times (5 minutes each) with wash buffer. Blots were hybridized with primary antibodies overnight at 4°C; membranes were washed 3 times (5 minutes each) and incubated with secondary antibodies (HRP conjugated). Bands were detected by using LumiGLO (Gaithersburg, MD) chemiluminescent substrate and Kodak (Rochester, NY) autoradiographic film. The intensities of specific immunoreactive bands were measured with Multi-Analyst v1.1 software (BIO-RAD). For immunoprecipitation studies, cell lysates (500 μg) were incubated overnight at 4°C with 5 μg of antibodies against either IR-β or IRS-1 and with constant agitation. Immunocomplexes were captured by adding 100 μL of Protein A agarose bead slurry (Upstate Biotechnology) and incubated for 2 hours at 4°C. Agarose beads were then washed 3 times with ice-cold PBS, resuspended in 50 μL of 2× Laemmli sample buffer (BIO-RAD), and boiled for 5 minutes. Supernatants were collected after pulse centrifugation and used in Western blotting, similar to the immunoblotting experiments mentioned above.

Reverse Transcription Polymerase Chain Reaction Assays

eNOS gene expression was determined by semi-quantitative reverse transcription polymerase chain reaction (RT-PCR) assays. Total RNA was extracted using TRIzol Reagent (Invitrogen, Carlsbad, CA) according to the manufacturer's instructions. Briefly, cells were cultured and treated in 60-mm culture dishes and lysed in 1.0 mL of TRIzol for 5 minutes, followed by the addition of 0.2 mL of chloroform. The mixture was shaken vigorously for 30 seconds, incubated for 3 minutes, and centrifuged at 12,000 × g for 15 minutes at 4°C. The top aqueous phase was removed and precipitated in an equal volume of isopropanol for 10 minutes at room temperature. The RNA pellet was obtained by centrifugation at 12,000 × g for 10 minutes at 4°C. The pellet was washed in 75% ethanol and centrifuged at 7,500 × g for 5 minutes. The RNA pellet was air dried, dissolved in diethylpyrocarbonate-treated water, and quantified using a

spectrophotometer. Aliquots were stored at −80°C for later use.

RT of 1 μg RNA was carried out at 42°C for 60 minutes in 20 μL of RT Mastermix containing 5 mM $MgCl_2$, 10 mM Tris-HCl (pH 8.3), 50 mM KCl, 1 mM dNTP, 1 U/μL RNase inhibitor, 2.5 U/μL cloned murine leukemia virus RT, and 2.5 μM oligo $(dT)_{16}$ as primer. PCR amplification of eNOS and glyceraldehyde 3 phosphate dehydrogenase (GAPDH) cDNAs was carried out using a GeneAmp PCR System 2400 (Applied Biosystems, Foster City, CA). The primers were synthesized by the Midland Certified Reagent Company (Midland, TX). The following primer sequences were used: eNOS,[47] upper 5′-GTG ATG GCG AAG CGA GTG AAG-3′ and lower 5′-CCG AGC CCG AAC ACA CAG AAC-3′ and GAPDH,[34] upper 5′-ACC ACA GTC CAT GCC ATC AC-3′ and lower 5′-TCC ACC ACC CTG TTG CTG TA-3′. The PCR Mastermix consisted of 2 μL cDNA, 2.0 mM $MgCl_2$, 0.2 mM dNTP, 0.5 U/25 μL AmpliTaq DNA polymerase, and 0.4 μM paired specific primers for eNOS or GAPDH in a total volume of 25 μL. The following conditions for PCR were used: 95°C for 2 minutes; 94°C for 1 minute, 60°C for 1 minute, 72°C for 1.5 minutes, 35 cycles; 72°C for 5 minutes. PCR products were separated by 2% agarose gel electrophoresis stained with ethidium bromide (0.5 μg/mL), and the expected product sizes for eNOS (422 bp) and GAPDH (452 bp) were visualized under ultraviolet light. The band intensities for PCR products were determined from scanned gel images by using the GS-700 Imaging Densitometer (BIO-RAD). Changes in eNOS expression were calculated by normalizing with GAPDH values.

Statistical Analysis

All statistical analyses were performed with the InStat v2 software (GraphPad Software, San Diego, CA). Experiments were performed at least 3-5 times, and the values obtained from 2-4 replicate samples were averaged in each experiment. Results are expressed as the standard error of the mean. Significant changes from controls were determined by using a 2-tailed Student *t* test, and comparisons among 3 or more groups were carried out by 1-way analysis of variance (ANOVA). For all tests, $P<0.05$ was considered significant.

RESULTS

Chronic Exposure to NEL Suppresses Insulin-Induced NO Production in HAECs

The effects of chronic exposure (72 hours) to physiological concentrations (<5 μg/mL) of NEL (0.25-2 μg/mL) on NO production by HAECs were determined. NEL was replenished every 24 hours, and the effects on both basal and insulin-induced NO production were monitored by 2 different fluorimetric assays for NO (Figures 1A and 1B). Fluorescent dye DAF-2 DA was used to visualize NO generation by immunofluorescence microscopy (A), and fluorimetric dye DAF-FM DA was used to quantitate intracellular NO levels (B). As observed in Figure 1A, insulin (100 ng/mL) stimulation for 10 minutes significantly increased the fluorescent intensity of cells. However, this intensity was much lower in cells chronically preexposed to NEL. The fluorescent reading in Figure 1B shows a 3- to 4-fold increase in NO production following insulin stimulation. Exposure to increasing concentrations of NEL suppressed this NO production. A concentration-dependent decrease in NO production was observed, and a significant ($P<0.05$) effect was seen even with low NEL concentrations (0.5 μg/mL). Higher NEL concentrations (1 and 2 μg/mL) suppressed basal NO production and fully abrogated insulin's inductive effect on NO production.

Chronic Exposure to NEL Decreases Insulin-Induced Akt and eNOS Phosphorylation in HAECs

Insulin stimulation causes a rapid increase in Akt phosphorylation at Ser473[38] and eNOS phosphorylation at Ser1177.[40] Western immunoblot studies showed that within 10 minutes of insulin (100 ng/mL) stimulation, Akt phosphorylation (p-Akt) increased by 3.5- to 4-fold (Figure 2A) and eNOS phosphorylation (p-eNOS) increased by 1.8- to 2-fold (Figure 2B). However, chronic preexposure to 1 or 2 μg/mL of NEL significantly suppressed this insulin-induced increase in p-Akt and p-eNOS levels in a dose-dependent manner. However, NEL exposure did not alter basal levels of either p-Akt and total Akt (tot-Akt) or p-eNOS and total eNOS (tot-eNOS) levels. Therefore, chronic NEL exposure suppressed insulin-induced Akt and eNOS phosphorylation, which may lead to the suppression of NO production in HAECs.

Chronic NEL Exposure Suppresses Activation of Second Messengers in the Insulin Signaling Cascade

Following insulin binding to its receptor, tyrosine phosphorylation of IR-β occurs, resulting in phosphorylation of IRS-1 followed by phosphorylation of the PI3K/p85α subunit and then Akt.[38,40] We monitored the effects of chronic NEL on downstream effectors of the insulin signaling cascade that leads to Akt phosphorylation (Figure 3). To facilitate the detection of IR-β and IRS-1, we first carried out immunoprecipitation using the respective antibodies. The immunoprecipitates were then used in

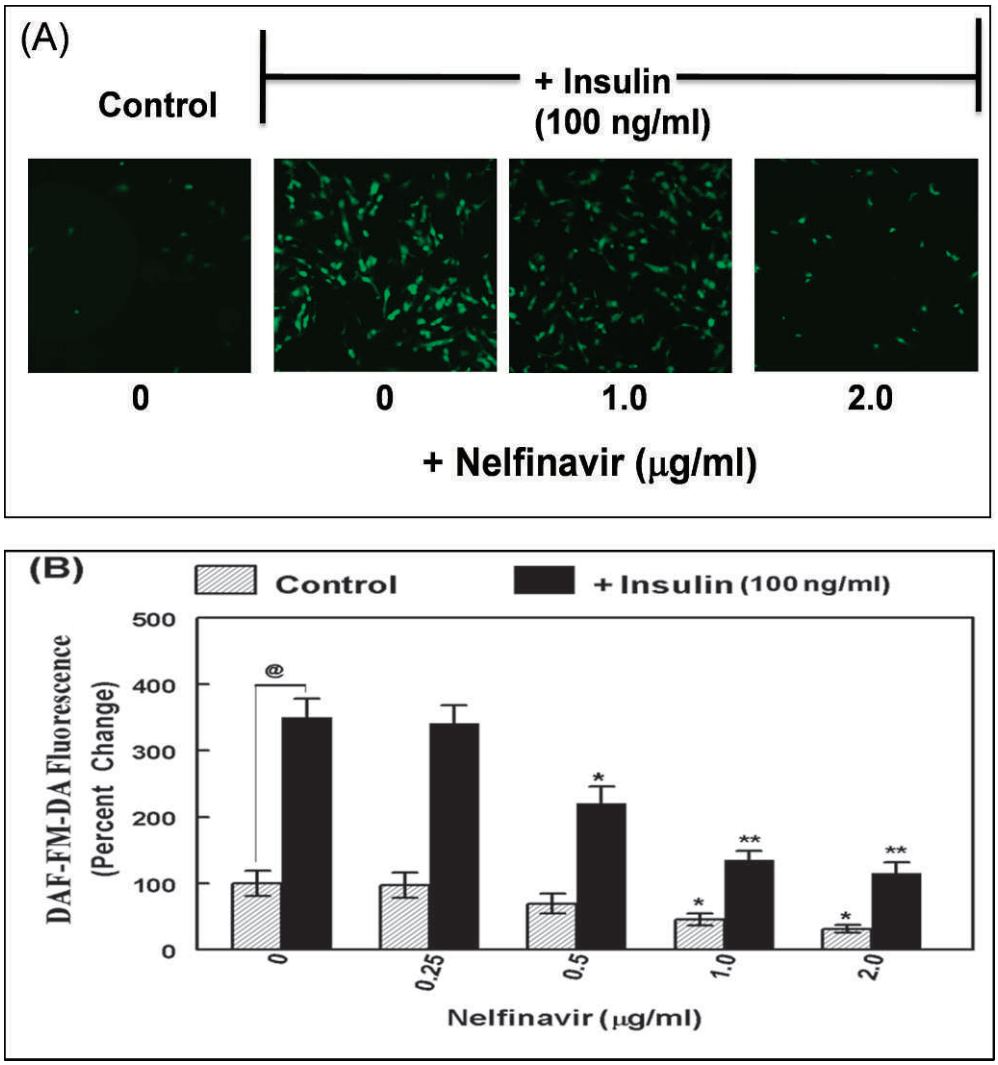

Figure 1. Effect of chronic exposure to nelfinavir (NEL) on insulin-induced nitric oxide (NO) production by human aortic endothelial cells. Cells were treated with NEL for a total of 72 hours with the drug replenished every 24 hours. Insulin (100 ng/mL) stimulation was carried out for the last 10 minutes prior to NO measurements. (A) Fluorescent dye DAF-2 DA was used to visualize NO generation by fluorescence microscopy. Increased fluorescence (green) in cells was observed within 10 minutes of insulin stimulation, but was much lower in cells preexposed to NEL. Microscopy images are representative of 3 independent experiments (n=3). (B) Fluorimetric dye DAF-FM DA was used to quantitate intracellular NO levels in real time. A percent increase in fluorescent intensity of cells was observed following insulin stimulation, but the increase was much lower in cells preexposed to NEL (0.25-2 μg/mL). Bar graph data represent the average of 4 independent experiments (n=4), and error bars represent the standard error of the mean (SEM). The @ represents significant ($P<0.005$) differences in NO levels in insulin-stimulated vs control cells. Significant decreases in both basal and insulin-stimulated NO were seen in cells exposed to NEL, shown as *$P<0.05$ and **$P<0.01$.

immunoblotting with an antibody that recognizes phosphorylated tyrosines. The detection of PI3K/p85α was carried out directly without prior immunoprecipitation. The fold changes for each of these phosphorylated proteins are shown in the bottom of each panel. Results clearly show that insulin stimulation increases (by 2- to 4-fold) the phosphorylation of IR-β, IRS-1, and PI3K/p85α. However, chronic preexposure to 1 or 2 μg/mL of NEL clearly suppressed the increase in these effectors of the insulin signaling cascade in a dose-dependent manner.

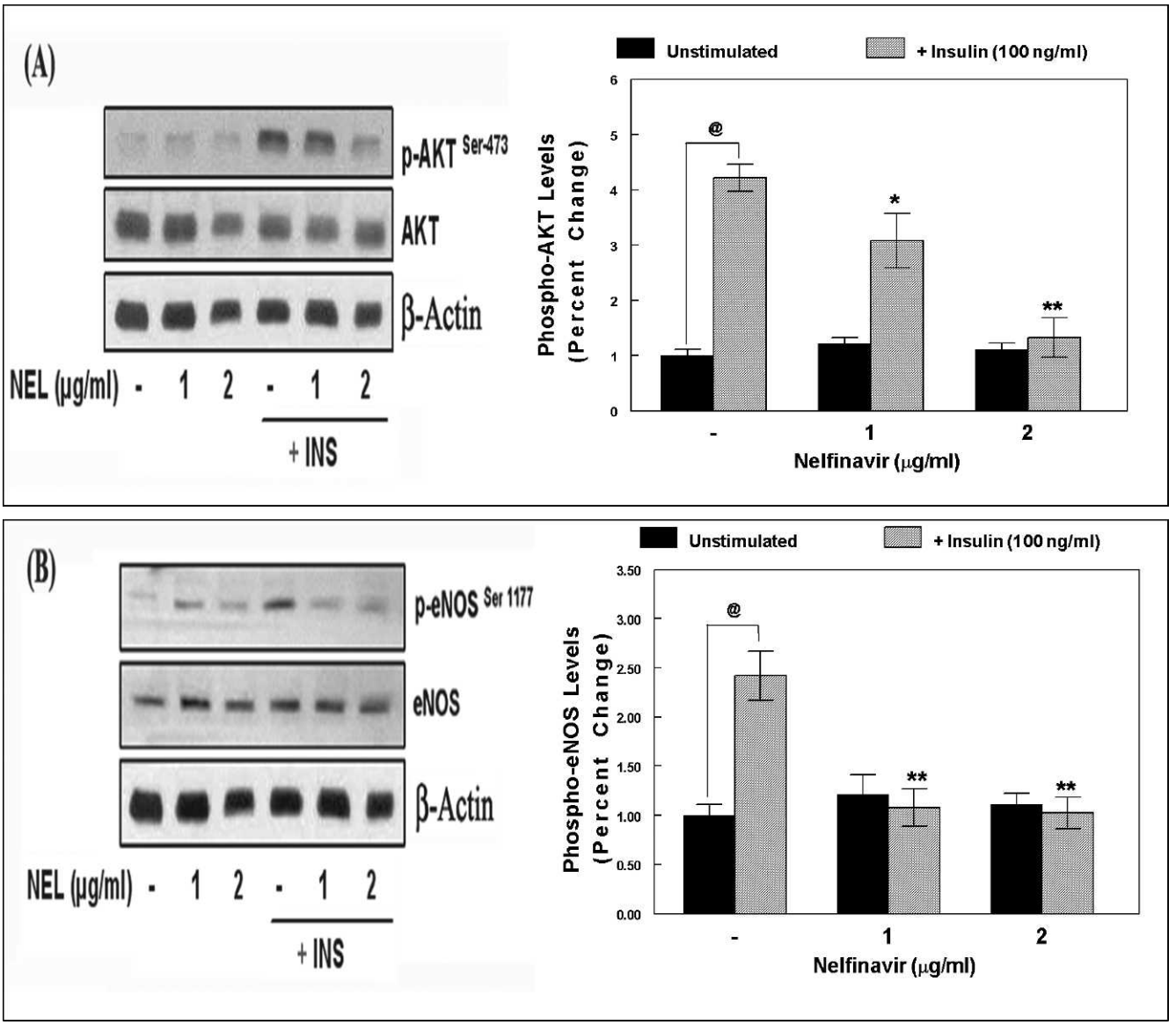

Figure 2. Effect of chronic nelfinavir (NEL) exposure on Akt and endothelial nitric oxide synthase (eNOS) activation in human aortic endothelial cells that were chronically treated with NEL (1 or 2 μg/mL) for 72 hours and then stimulated with or without insulin (INS) (100 ng/mL) for 10 minutes. Cells were harvested, and cell extracts were used in Western blot for total Akt and eNOS, as well as phosphorylated Akt (p-Akt) (serine residue [Ser]473) or phosphorylated eNOS (p-eNOS) (Ser1177). A representative autoradiogram is shown on the left panel. Bar graphs on the right show fold changes in (A) p-Akt and (B) p-eNOS levels, compared with basal controls. Densitometric values for bands were normalized to β-actin levels in respective samples. Data represent the average of 3 independent experiments (n=3), and error bars represent the standard error of the mean. The @ represents significant ($P<0.005$) differences in p-Akt or p-eNOS levels in insulin-stimulated cells vs control cells. Significant decreases in both basal and insulin-stimulated Akt and eNOS activation (phosphorylation) were seen in cells exposed to NEL: *$P<0.05$ and **$P<0.01$.

Insulin Sensitization via TRO Overcomes the Suppressive Effects of NEL on p-Akt and p-eNOS

The PPAR-γ agonists, TZDs, increase insulin sensitivity of cells.[41] TRO is one of the most potent of the clinically approved TZDs. Thus, we wanted to determine whether exposure to TRO can ameliorate the deleterious effects of NEL. Similar to previous experiments, HAECs were chronically (72 hours) exposed to NEL (1 or 2 μg/mL) in the presence or absence of TRO (250 nM), and both drugs were

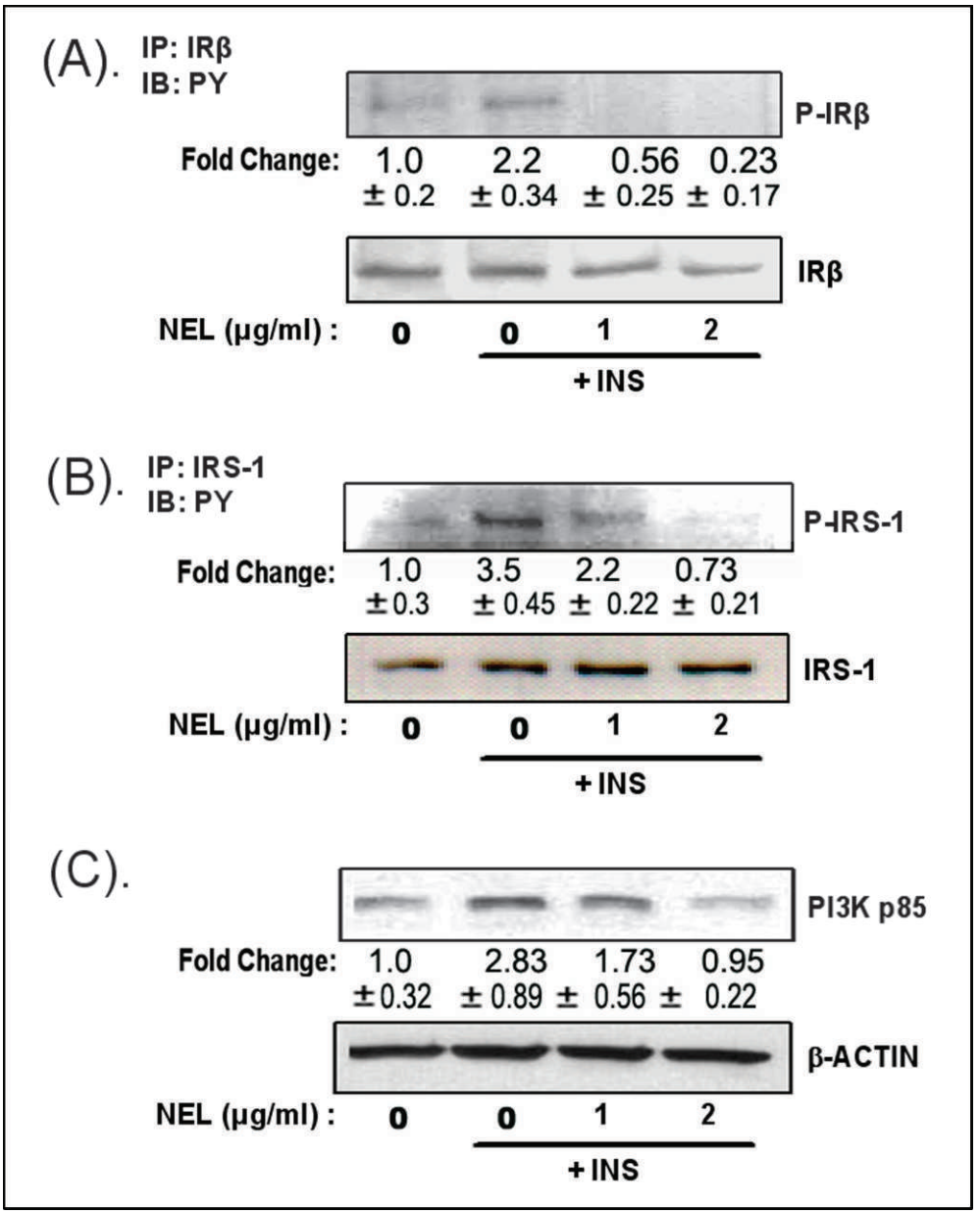

Figure 3. Effect of chronic nelfinavir (NEL) exposure on the activation of second messengers of the insulin (INS) signaling cascade. We monitored the effects of chronic NEL on downstream effectors of the insulin signaling cascade: (A) insulin receptor beta (IR-β), (B) insulin receptor substrate-1 (IRS-1), and (C) PI3K/p85α. For phosphorylated IR-β or IRS-1 detection, proteins were first immunoprecipitated (IP) using the respective antibodies, electrophoresed on SDS-PAGE gel, and immunoblotted (IB) with an antibody against phosphorylated tyrosines (PY). The detection of PI3K/p85α was carried out directly. The fold changes for each of these phosphorylated proteins are shown at the bottom of each panel. Densitometric values for each band were normalized to β-actin levels in respective samples. Data represent the average of 3 independent experiments (n=3), and error bars represent the standard error of the mean. Insulin stimulation increased phosphorylation of IR-β, IRS-1, and PI3K/p85α. Chronic preexposure to NEL (1 or 2 μg/mL) suppressed these increases in insulin signaling effectors.

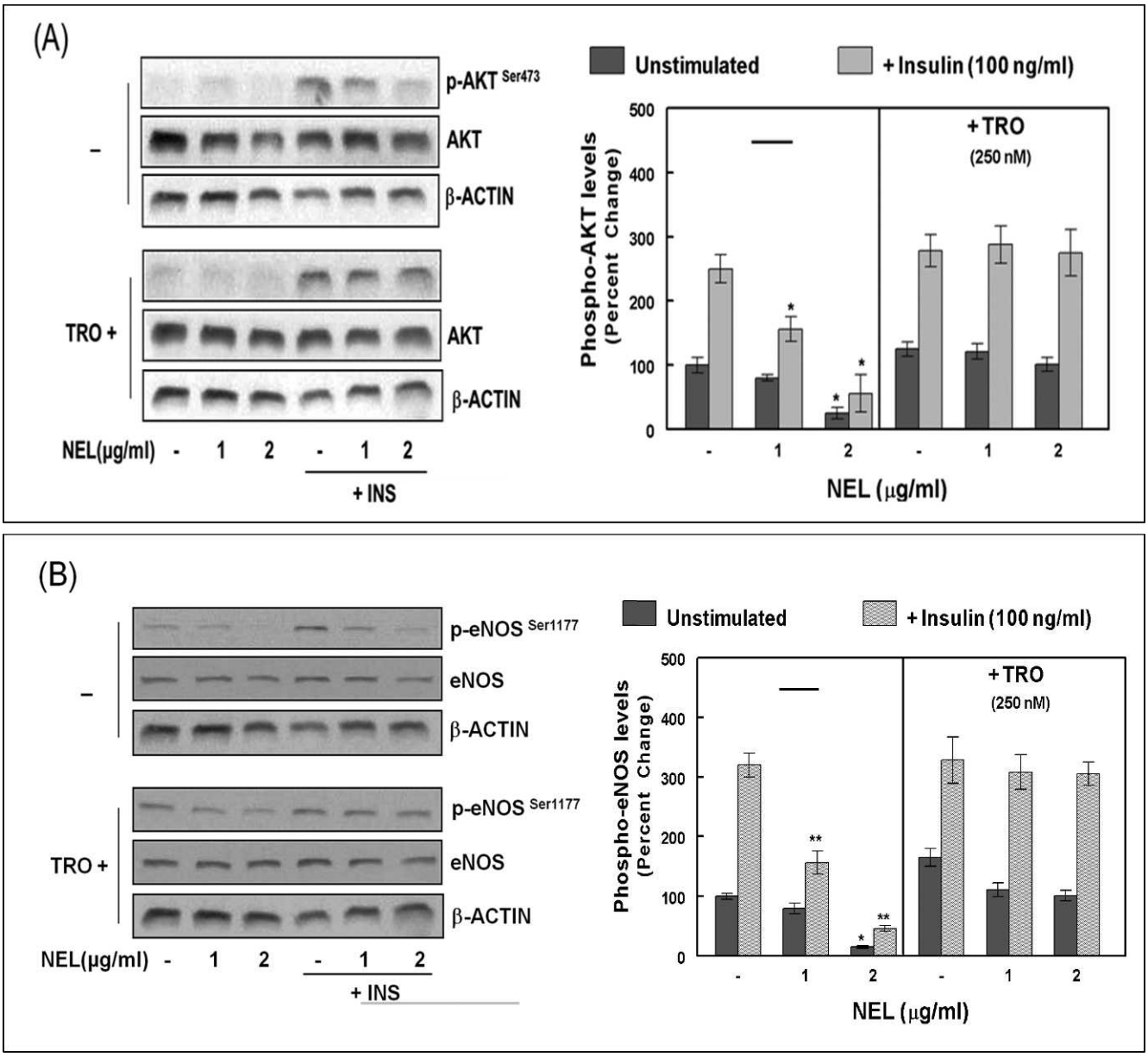

Figure 4. Effect of troglitazone (TRO) cotreatment on nelfinavir (NEL)-mediated suppression of Akt and endothelial nitric oxide synthase (eNOS) phosphorylation. We determined whether coexposure to TRO can ameliorate the deleterious effects of NEL in HAECs that were chronically (72 hours) exposed to NEL (1 or 2 μg/mL) in the presence or absence of TRO (250 nM). Following insulin (INS) (100 ng/mL) stimulation for 15 minutes, inductions in Akt and eNOS phosphorylation were monitored by Western blot. A representative autoradiogram is shown on the left panel. Bar graphs on the right show percent changes in (A) phosphorylated Akt (p-Akt) (serine residue [Ser]473) and (B) phosphorylated eNOS (p-eNOS) (Ser1177) levels compared with basal controls. Densitometric values for each band were normalized to β-actin levels in respective samples. Data represent the average of 3 independent experiments (n=3), and error bars represent the standard error of the mean. The differences in p-Akt or p-eNOS levels in the presence or absence of TRO stimulation are shown. Significant decreases in both basal and insulin-stimulated Akt and eNOS phosphorylation were seen in cells exposed to NEL (*$P<0.05$ and **$P< 0.01$) but were not observed in TRO-exposed cells.

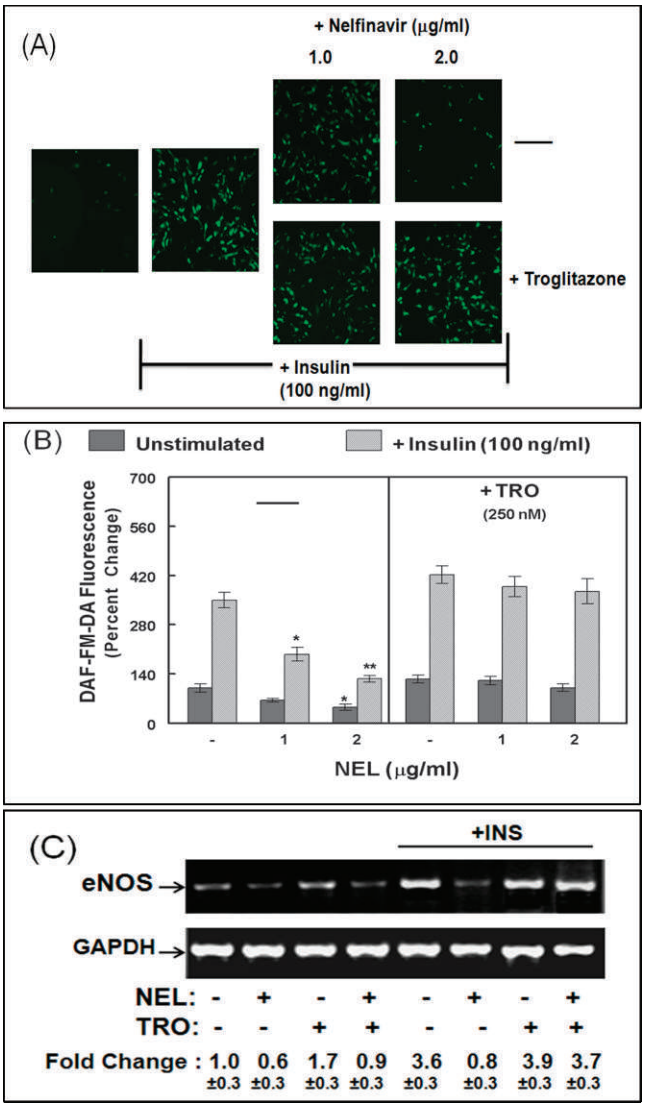

Figure 5. Effect of troglitazone (TRO) cotreatment on nelfinavir (NEL)-mediated suppression of nitric oxide (NO) production and endothelial NO synthase (eNOS) gene expression in insulin (INS)-stimulated human aortic endothelial cells (HAECs). The effect of chronic NEL exposure on NO production in HAECs was monitored in the presence or absence of TRO cotreatment by (A) fluorescent dye DAF-2 DA fluorescence microscopy and (B) fluorimetric dye DAF-FM DA fluorimetry. The effect of chronic NEL exposure on insulin-induced eNOS gene expression in the presence or absence of TRO cotreatment was monitored by (C) semiquantitative reverse transcription polymerase chain reaction. (A) A representative image of fluorescence shows that cells chronically exposed to NEL produce less NO in response to insulin stimulation, an effect that was ameliorated by TRO. (B) The NO assay showed that the insulin-stimulated increase in fluorescent intensity is much lower in cells chronically exposed to NEL but not in TRO coexposed cells. Bar graph data represent the average of 3 independent experiments (n=3), and error bars represent the standard error of the mean. Significant decreases are shown as *$P<0.05$ and **$P<0.01$. (C) Representative (n=4) gel pictures for polymerase chain reaction (PCR) products of eNOS and glyceraldehyde 3-phosphate dehydrogenase (GAPDH) are shown. Fold changes in insulin-stimulated eNOS gene expression, compared with basal controls and following normalization with GAPDH messenger RNA levels, are provided at the bottom of each panel. TRO coexposure was able to overcome the suppressive effect of NEL on insulin-induced eNOS gene expression.

replenished every 24 hours. Following insulin (100 ng/mL) stimulation for 15 minutes, induction of Akt and eNOS phosphorylation was monitored by Western blot (Figure 4). Our data clearly show that NEL significantly suppressed both p-Akt (3- to 4-fold) and p-eNOS (5- to 6-fold) levels. However, this suppression was not observed in TRO coexposed cells. TRO alone did not alter the levels of non-phosphorylated forms of Akt and eNOS, either under basal or insulin-induced conditions. Furthermore, compared with control cells, insulin-induced p-Akt and p-eNOS levels were not different in TRO-treated cells. This research clearly suggests that TRO treatment can ameliorate the suppressive effects of NEL and that this effect is not caused by an increase in tot-Akt or tot-eNOS protein levels but rather by an increase in the phosphorylation of these 2 proteins that are known to regulate NO production in ECs.

TRO Treatment Overcomes the Effect of NEL on Insulin-Induced NO Production and eNOS Expression

Similar to previous studies, we monitored the effect of chronic NEL exposure in HAECs in the presence or absence of TRO cotreatment (Figure 5). Following acute exposure (15 minutes) to insulin, NO production was measured by both (A) DAF-2 DA fluorescence microscopy and (B) DAF-FM DA fluorimetry. We also measured the long-term (8 hours) effects of insulin on eNOS gene expression by RT-PCR and determined whether chronic NEL exposure in the presence or absence of TRO cotreatment has an effect on (C) eNOS messenger RNA (mRNA) levels. As shown in the images in Figure 5A, chronic NEL exposure decreased insulin-induced NO production. However, TRO coexposure ameliorated this decrease in fluorescence intensity of cells. In Figure 5B, intracellular NO quantitation results show that exposure to NEL (2 μg/mL) severely suppressed insulin-induced NO production. TRO coexposure overcame this effect under both basal and insulin-stimulated conditions. In Figure 5C, the fold changes in eNOS gene expression show that eNOS mRNA increased by 3- to 4-fold after 8 hours of insulin stimulation but was significantly decreased in NEL-exposed cells. In control cells, TRO exposure slightly increased basal eNOS mRNA levels but did not have any detectable effects on insulin-stimulated eNOS expression. However, in NEL-exposed cells, TRO cotreatment upregulated insulin-induced eNOS gene expression, almost to the level seen in control cells. Thus, our findings demonstrate that a potent TZD like TRO may have significant protective effects against chronic exposure to NEL in HAECs.

DISCUSSION

Because ECs are chronically exposed to high concentrations of PIs in HIV-1–positive patients, endothelial dysfunction may play a direct role in the progression of vascular disease and atherosclerosis.[15,27,34] Findings indicate that PIs may manifest these deleterious effects because of the induction of oxidative stress that leads to endothelial activation, recruitment of leukocytes and platelets, and dysregulation in the expression of EDRFs. Furthermore, the accumulation of oxidized low-density lipoproteins in subendothelial spaces may eventually lead to acute coronary events and thrombus formation in these patients. Indeed, the effects of hyperinsulinemia, hyperglycemia, and adipokine release may play a direct role in the pathogenesis of vascular disease in the setting of chronic HAART. Because of lipodystrophy and increased levels of triglycerides in HIV-positive individuals on HAART, adipokines may also be significant risk factors for vascular disease. However, Kaneki and colleagues[48] in 2009 indicated that insulin resistance and oxidative stress, rather than hyperinsulinemia or lipid disturbances themselves, may decrease vascular function in patients with diabetes. In cultured bovine ECs, high glucose levels inhibited eNOS phosphorylation at Ser1177,[49] suggesting that the relative deficiency in the action of insulin and concomitant hyperglycemia may operate together to cause impairments in Akt activity and NO production. Thus, impairments of insulin-induced PI3K/Akt activity and eNOS phosphorylation observed in type 2 diabetic mice may be secondary to insulin resistance. However, which missing action of insulin is responsible for PI-induced dysfunction in aortic ECs remains unclear. Our in vitro studies clearly indicate that NEL directly impairs the insulin signaling pathway, resulting in decreased Akt and eNOS phosphorylation and NO production.

Compared to patients on non-PI–based regimens, a significant reduction of flow-mediated vasodilation in HIV-infected patients receiving PIs was clearly evident.[15,16,22] Chai et al[50] investigated and compared the effects of 5 commonly used PIs (ritonavir, amprenavir, saquinavir, indinavir, and NEL) on vasomotor function, eNOS expression, and oxidative stress. The eNOS mRNA levels and NO production were significantly reduced with ritonavir, amprenavir, and saquinavir, but not with indinavir or NEL, even at the 15 μg/mL concentrations used. Furthermore, superoxide anion levels were significantly increased. The antioxidant seleno-L-methionine reversed ritonavir-induced superoxide production. However, in our investigations with human ECs, NEL had the highest suppressive effect on insulin-induced NO production and p-Akt levels compared with other PIs such as

ritonavir or saquinavir (data not shown). Furthermore, unlike our in vitro studies, these previous studies exposed ECs to supraphysiological concentrations (>5 μg/mL) of NEL and did not measure the effects of chronic exposure to physiological doses of NEL, unlike our current study in which drugs were replenished every day for 3 days.

Investigators have shown that NEL impairs insulin signaling by inducing oxidative stress in 3T3-L1 adipocytes, and exposure to the superoxide dismutase-mimetic antioxidant MnTBAP protected against impairment in insulin-stimulated Akt phosphorylation[51] via impaired plasma membrane recruitment of Akt.[52] These investigators[51] used a concentration as high as 30 μM (~18 μg/mL) NEL for 18 hours and evaluated the phosphorylation and localization of key proteins in the insulin signaling cascade. Interestingly, insulin-induced interaction of PI3K/p85α with IRS proteins 1 and 2 was normal in adipocytes treated with NEL, yet insulin-induced phosphorylation of Akt and extracellular signal-regulated kinase 1/2 was significantly impaired. The above investigators concluded that in adipocytes, NEL induces a defect in the insulin signaling cascade downstream of the activation of PI3K. However, our findings in HAECs clearly indicate that insulin-induced phosphorylation of upstream effectors, both IR-β and IRS-1, was suppressed in cells chronically exposed to NEL. This discrepancy may be caused by differences in NEL concentrations, ie, <5 μM (or <3 μg/mL) used in our study vs 30 μM (or 18 μg/mL) used in the previous studies. Furthermore, the cell type investigated (endothelial vs adipocytes) and the treatment conditions used (chronic and long term vs acute and short term) may also be factors that lead to differences in NEL's effects on insulin signaling. In our previous studies,[34] we observed that the antioxidants N-acetyl cysteine and glutathione, as well as the NO-donor sodium nitroprusside, were able to suppress PI-induced endothelial dysfunction, as measured by an increase in both leukocyte adhesion and cell adhesion molecule expression in HAECs. In the current study, we clearly show that chronic exposure to physiologically achievable concentrations of NEL can suppress NO production and manifest insulin resistance in HAECs.

The most important effect of Akt stimulation in the vascular system is its involvement in NO production via eNOS phosphorylation at Ser1177.[49] Therefore, we measured insulin-induced phosphorylation at this Akt-dependent site of eNOS. Furthermore, although threonine-308 phosphorylation is also necessary for Akt activation, Ser473 phosphorylation is crucial for maximal activity of Akt.[39] Therefore, we measured insulin-induced Ser473 phosphorylation of Akt. Our in vitro findings show that the potent PPAR-γ agonist TRO can suppress the deleterious effects of NEL on both p-Akt and p-eNOS levels in insulin-stimulated HAECs.

Several TZDs—TRO, ciglitazone, and rosiglitazone—reversed PI-induced inhibition of adipocyte differentiation and were implicated as potential drugs for treating lipoatrophy in HIV-positive patients.[53,54] The TZDs induced significant changes in gene expression in subcutaneous adipose tissue and ameliorated insulin resistance in patients with lipodystrophy. Gavrila et al[55] in 2005 showed that 12-month treatment with pioglitazone, but not with the PPAR-α agonist fenofibrate, was able to improve HAART-induced metabolic syndrome, insulin resistance, blood pressure, and lipid profiles in HIV-infected patients. We present data for only TRO, known to be one of the most potent of the TZDs,[56] but discontinued because of its significant liver toxicities.[44] Our studies showed that several other TZDs, such as rosiglitazone and ciglitazone, can also manifest similar protective effects on HAECs. However, at least 8- to 10-fold higher concentrations compared to the concentration of TRO (250 nM) were needed to suppress the deleterious effects of chronic NEL exposure (data not shown).

Although the metabolic side effects have not been severe with the newer PIs such as lopinavir and darunavir, the older PIs are still part of the HAART regimen, especially in resource-poor settings. Furthermore, because ritonavir is an inhibitor of the CYP450 system, low-dose ritonavir is regularly used with another PI in a ritonavir-boosted regimen. Thus, cardiovascular dysfunction associated with PIs will most likely persist in HIV-infected patients, and a better understanding of their mechanisms of action and applicability of adjunct therapy to suppress these side effects will be of significant clinical benefit. Lastly, several of the older PIs are being repositioned as anticancer agents, as evident from numerous recent clinical trials.[13,14,40] NEL is a broad-spectrum antitumor agent that induces endoplasmic reticulum stress and autophagy and suppresses Akt and other survival pathways in tumor cells.[57] NEL also can augment the antitumor efficacy of other chemotherapeutic agents.[58] Therefore, the metabolic effects of chronic exposure to NEL may likely be manifested in patients with cancer, and the protective effects of TZDs may be of great clinical benefit to them as well.

CONCLUSION

A number of previous investigations showed that TZDs may provide significant benefits by suppressing the development of cancers[59] and acting as chemo-

sensitizing agents.[60] Therefore, our current findings provide novel insights, not only toward the therapeutic management of NEL-induced side effects in HIV-infected patients by adjunct treatment with TZDs, but also regarding the possible utility of TZDs in future combinatorial strategies with NEL to exacerbate the cytotoxic effects on tumor cells and simultaneously ameliorate the metabolic side effects of NEL on normal cells. Therefore, our findings suggest that adjunct therapy with insulin sensitizers may protect against the endothelial dysfunctions observed during long-term HAART exposure in HIV-1 infected individuals.

REFERENCES

1. Arts EJ, Hazuda DJ. HIV-1 antiretroviral drug therapy. *Cold Spring Harb Perspect Med*. 2012 Apr;2(4):a007161.
2. Palella FJ Jr, Delaney KM, Moorman AC, et al. Declining morbidity and mortality among patients with advanced human immunodeficiency virus infection. HIV Outpatient Study Investigators. *N Engl J Med*. 1998 Mar 26;338(13):853-860.
3. May MT, Sterne JA, Costagliola D, et al; Antiretroviral Therapy (ART) Cohort Collaboration. HIV treatment response and prognosis in Europe and North America in the first decade of highly active antiretroviral therapy: a collaborative analysis. *Lancet*. 2006 Aug 5;368(9534):451-458.
4. Moreno S, López Aldeguer J, Arribas JR, et al; HIV 2020 Project. The future of antiretroviral therapy: challenges and needs. *J Antimicrob Chemother*. 2010 May;65(5):827-835. Epub 2010 Mar 12.
5. Mulligan K, Grunfeld C, Tai VW, et al. Hyperlipidemia and insulin resistance are induced by protease inhibitors independent of changes in body composition in patients with HIV infection. *J Acquir Immune Defic Syndr*. 2000 Jan 1;23(1):35-43.
6. Galli M, Ridolfo AL, Adorni F, et al. Body habitus changes and metabolic alterations in protease inhibitor-naive HIV-1-infected patients treated with two nucleoside reverse transcriptase inhibitors. *J Acquir Immune Defic Syndr*. 2002 Jan 1;29(1):21-31.
7. Holmberg SD, Moorman AC, Williamson JM, et al; HIV Outpatient Study (HOPS) investigators. Protease inhibitors and cardiovascular outcomes in patients with HIV-1. *Lancet*. 2002 Nov 30;360(9347):1747-1748.
8. Ellis RJ, Marquie-Beck J, Delaney P, et al; CHARTER Group. Human immunodeficiency virus protease inhibitors and risk for peripheral neuropathy. *Ann Neurol*. 2008 Nov;64(5):566-572.
9. Coleman CI, White CM. A comparison of different protease inhibitors on coronary heart disease risk. *Conn Med*. 2007 Jan; 71(1):15-17.
10. Hunt K, Hughes CA, Hills-Nieminen C. Protease inhibitor-associated QT interval prolongation. *Ann Pharmacother*. 2011 Dec;45(12):1544-1550. Epub 2011 Nov 29.
11. Chandra S, Mondal D, Agrawal KC. HIV-1 protease inhibitor induced oxidative stress suppresses glucose stimulated insulin release: protection with thymoquinone. *Exp Biol Med (Maywood)*. 2009 Apr;234(4):442-453. Epub 2009 Feb 20.
12. Worm SW, Sabin C, Weber R, et al. Risk of myocardial infarction in patients with HIV infection exposed to specific individual antiretroviral drugs from the 3 major drug classes: the data collection on adverse events of anti-HIV drugs (D:A:D) study. *J Infect Dis*. 2010 Feb 1;201(3):318-330.
13. Rengan R, Mick R, Pryma D, et al. A phase I trial of the HIV protease inhibitor nelfinavir with concurrent chemoradiotherapy for unresectable stage IIIA/IIIB non-small cell lung cancer: a report of toxicities and clinical response. *J Thorac Oncol*. 2012 Apr;7(4): 709-715.
14. Brunner TB, Geiger M, Grabenbauer GG, et al. Phase I trial of the human immunodeficiency virus protease inhibitor nelfinavir and chemoradiation for locally advanced pancreatic cancer. *J Clin Oncol*. 2008 Jun 1;26(16):2699-2706.
15. Stein JH, Klein MA, Bellehumeur JL, et al. Use of human immunodeficiency virus-1 protease inhibitors is associated with atherogenic lipoprotein changes and endothelial dysfunction. *Circulation*. 2001 Jul 17;104(3):257-262.
16. Rhew DC, Bernal M, Aguilar D, Iloeje U, Goetz MB. Association between protease inhibitor use and increased cardiovascular risk in patients infected with human immunodeficiency virus: a systematic review. *Clin Infect Dis*. 2003 Oct 1;37(7):959-972. Epub 2003 Sep 12.
17. Henry K, Melroe H, Huebesch J, Hermundson J, Simpson J. Atorvastatin and gemfibrozil for protease-inhibitor-related lipid abnormalities. *Lancet*. 1998 Sep 26;352(9133):1031-1032.
18. Aberg JA, Zackin RA, Brobst SW, et al; ACTG 5087 Study Team. A randomized trial of the efficacy and safety of fenofibrate versus pravastatin in HIV-infected subjects with lipid abnormalities: AIDS Clinical Trials Group Study 5087. *AIDS Res Hum Retroviruses*. 2005 Sep;21(9):757-767.
19. Giannarelli C, Klein RS, Badimon JJ. Cardiovascular implications of HIV-induced dyslipidemia. *Atherosclerosis*. 2011 Dec;219(2): 384-389. Epub 2011 Jun 13.
20. Klein D, Hurley LB, Quesenberry CP Jr, Sidney S. Do protease inhibitors increase the risk for coronary heart disease in patients with HIV-1 infection? *J Acquir Immune Defic Syndr*. 2002 Aug 15;30(5):471-477.
21. Blanco F, San Román J, Vispo E, et al. Management of metabolic complications and cardiovascular risk in HIV-infected patients. *AIDS Rev*. 2010 Oct-Dec;12(4):231-241.
22. Silic A, Janez A, Tomazic J, et al. Effect of rosiglitazone and metformin on insulin resistance in patients infected with human immunodeficiency virus receiving highly active antiretroviral therapy containing protease inhibitor: randomized prospective controlled clinical trial. *Croat Med J*. 2007 Dec; 48(6):791-799.
23. Bonetti PO, Lerman LO, Lerman A. Endothelial dysfunction: a marker of atherosclerotic risk. *Arterioscler Thromb Vasc Biol*. 2003 Feb 1;23(2):168-175.
24. Hadi HA, Carr CS, Al Suwaidi J. Endothelial dysfunction: cardiovascular risk factors, therapy, and outcome. *Vasc Health Risk Manag*. 2005;1(3):183-198.
25. Bozzette SA, Ake CF, Tam HK, Chang SW, Louis TA. Cardiovascular and cerebrovascular events in patients treated for human immunodeficiency virus infection. *N Engl J Med*. 2003 Feb 20;348(8):702-710.
26. Bevilacqua M, Dominguez LJ, Barbagallo M. Insulin resistance and the cardiometabolic syndrome in HIV infection. *J Cardiometab Syndr*. 2009 Winter;4(1):40-43.
27. Mondy KE, de las Fuentes L, Waggoner A, et al. Insulin resistance predicts endothelial dysfunction and cardiovascular risk in HIV-infected persons on long-term highly active antiretroviral therapy. *AIDS*. 2008 Apr 23;22(7):849-856.

28. Schillaci G, De Socio GV, Pucci G, et al. Aortic stiffness in untreated adult patients with human immunodeficiency virus infection. *Hypertension*. 2008 Aug;52(2):308-313. Epub 2008 Jun 16.
29. Sugawara J, Komine H, Hayashi K, et al. Effect of systemic nitric oxide synthase inhibition on arterial stiffness in humans. *Hypertens Res*. 2007 May;30(5):411-415.
30. Papita A, Albu A, Fodor D, Itu C, Cârstina D. Arterial stiffness and carotid intima-media thickness in HIV infected patients. *Med Ultrason*. 2011 Jun;13(2):127-134.
31. Flammer AJ, Lüscher TF. Human endothelial dysfunction: EDRFs. *Pflugers Arch*. 2010 May;459(6):1005-1013. Epub 2010 Apr 12.
32. Kim JA, Montagnani M, Koh KK, Quon MJ. Reciprocal relationships between insulin resistance and endothelial dysfunction: molecular and pathophysiological mechanisms. *Circulation*. 2006 Apr 18;113(15):1888-1904.
33. Muller G, Goettsch C, Morawietz H. Oxidative stress and endothelial dysfunction. *Hamostaseologie*. 2007 Feb;27(1):5-12.
34. Mondal D, Pradhan L, Ali M, Agrawal KC. HAART drugs induce oxidative stress in human endothelial cells and increase endothelial recruitment of mononuclear cells: exacerbation by inflammatory cytokines and amelioration by antioxidants. *Cardiovasc Toxicol*. 2004;4(3):287-302.
35. Jiang B, Hebert VY, Khandelwal AR, Stokes KY, Dugas TR. HIV-1 antiretrovirals induce oxidant injury and increase intima-media thickness in an atherogenic mouse model. *Toxicol Lett*. 2009 Jun 22;187(3):164-171. Epub 2009 Mar 9.
36. Touzet O, Philips A. Resveratrol protects against protease inhibitor-induced reactive oxygen species production, reticulum stress and lipid raft perturbation. *AIDS*. 2010 Jun 19;24(10): 1437-1447.
37. Wang X, Chai H, Lin PH, Yao Q, Chen C. Roles and mechanisms of human immunodeficiency virus protease inhibitor ritonavir and other anti-human immunodeficiency virus drugs in endothelial dysfunction of porcine pulmonary arteries and human pulmonary artery endothelial cells. *Am J Pathol*. 2009 Mar;174(3):771-781. Epub 2009 Feb 13.
38. Jensen M, De Meyts P. Molecular mechanisms of differential intracellular signaling from the insulin receptor. *Vitam Horm*. 2009;80:51-75.
39. Vasudevan KM, Garraway LA. AKT signaling in physiology and disease. *Curr Top Microbiol Immunol*. 2010;347:105-133.
40. Plastaras JP, Vapiwala N, Ahmed MS, et al. Validation and toxicity of PI3K/Akt pathway inhibition by HIV protease inhibitors in humans. *Cancer Biol Ther*. 2008 May;7(5):628-635. Epub 2008 May 14.
41. Balakumar P, Kathuria S. Submaximal PPARγ activation and endothelial dysfunction: new perspectives for the management of cardiovascular disorders. *Br J Pharmacol*. 2012 Aug;166(7): 1981-1992.
42. Schmidt MV, Brüne B, von Knethen A. The nuclear hormone receptor PPARγ as a therapeutic target in major diseases. *ScientificWorldJournal*. 2010 Nov 4;10:2181-2197.
43. Hamblin M, Chang L, Fan Y, Zhang J, Chen YE. PPARs and the cardiovascular system. *Antioxid Redox Signal*. 2009 Jun;11(6): 1415-1452.
44. Cariou B, Charbonnel B, Staels B. Thiazolidinediones and PPARγ agonists: time for a reassessment. *Trends Endocrinol Metab*. 2012 May;23(5):205-215. Epub 2012 Apr 17.
45. Zhou X, He P. Improved measurements of intracellular nitric oxide in intact microvessels using 4,5-diaminofluorescein diacetate. *Am J Physiol Heart Circ Physiol*. 2011 Jul;301(1):H108-H114. Epub 2011 May 2.
46. Sheng JZ, Wang D, Braun AP. DAF-FM (4-amino-5-methylamino-2′,7′-difluorofluorescein) diacetate detects impairment of agonist-stimulated nitric oxide synthesis by elevated glucose in human vascular endothelial cells: reversal by vitamin C and L-sepiapterin. *J Pharmacol Exp Ther*. 2005 Nov;315(2):931-940. Epub 2005 Aug 10.
47. Pradhan L, Mondal D, Chandra S, Ali M, Agrawal KC. Molecular analysis of cocaine-induced endothelial dysfunction: role of endothelin-1 and nitric oxide. *Cardiovasc Toxicol*. 2008 Dec;8(4): 161-171. Epub 2008 Sep 24.
48. Kaneki M, Shinozaki S, Chang K, Shimizu N. Could insulin sensitization be used as an alternative to intensive insulin therapy to improve the survival of intensive care unit patients with stress-induced hyperglycemia? *Crit Care Med*. 2009 Oct;37(10):2856-2858.
49. Du XL, Edelstein D, Dimmeler S, Ju Q, Sui C, Brownlee M. Hyperglycemia inhibits endothelial nitric oxide synthase activity by posttranslational modification at the Akt site. *J Clin Invest*. 2001 Nov;108(9):1341-1348.
50. Chai H, Yang H, Yan S, et al. Effects of 5 HIV protease inhibitors on vasomotor function and superoxide anion production in porcine coronary arteries. *J Acquir Immune Defic Syndr*. 2005 Sep 1;40(1):12-19.
51. Ben-Romano R, Rudich A, Etzion S, et al. Nelfinavir induces adipocyte insulin resistance through the induction of oxidative stress: differential protective effect of antioxidant agents. *Antivir Ther*. 2006;11(8):1051-1060.
52. Ben-Romano R, Rudich A, Tirosh A, et al. Nelfinavir-induced insulin resistance is associated with impaired plasma membrane recruitment of the PI 3-kinase effectors Akt/PKB and PKC-zeta. *Diabetologia*. 2004 Jun;47(6):1107-1117. Epub 2004 May 28.
53. Caron M, Vigouroux C, Bastard JP, Capeau J. Antiretroviral-related adipocyte dysfunction and lipodystrophy in HIV-infected patients: Alteration of the PPARγ-dependent pathways. *PPAR Res*. 2009;2009:507141. Epub 2008 Dec 30.
54. Sutinen J. The effects of thiazolidinediones on metabolic complications and lipodystrophy in HIV-infected patients. *PPAR Res*. 2009;2009:373524. Epub 2008 Dec 1.
55. Gavrila A, Hsu W, Tsiodras S, et al. Improvement in highly active antiretroviral therapy-induced metabolic syndrome by treatment with pioglitazone but not with fenofibrate: a 2×2 factorial, randomized, double-blinded, placebo-controlled trial. *Clin Infect Dis*. 2005 Mar 1;40(5):745-749. Epub 2005 Feb 7.
56. Nolan JJ, Ludvik B, Beerdsen P, Joyce M, Olefsky J. Improvement in glucose tolerance and insulin resistance in obese subjects treated with troglitazone. *N Engl J Med*. 1994 Nov 3;331(18): 1188-1193.
57. Gills JJ, Lopiccolo J, Tsurutani J, et al. Nelfinavir, A lead HIV protease inhibitor, is a broad-spectrum, anticancer agent that induces endoplasmic reticulum stress, autophagy, and apoptosis in vitro and in vivo. *Clin Cancer Res*. 2007 Sep 1;13(17):5183-5194.
58. Kawabata S, Gills JJ, Mercado-Matos JR, et al. Synergistic effects of nelfinavir and bortezomib on proteotoxic death of NSCLC and multiple myeloma cells. *Cell Death Dis*. 2012 Jul 19; 3:e353.

59. Han S, Roman J. Peroxisome proliferator-activated receptor gamma: a novel target for cancer therapeutics? *Anticancer Drugs*. 2007 Mar;18(3):237-244.

60. Yokoyama Y, Xin B, Shigeto T, Mizunuma H. Combination of ciglitazone, a peroxisome proliferator-activated receptor gamma ligand, and cisplatin enhances the inhibition of growth of human ovarian cancers. *J Cancer Res Clin Oncol*. 2011 Aug;137(8): 1219-1228. Epub 2011 Jun 17.

This article meets the Accreditation Council for Graduate Medical Education and the American Board of Medical Specialties Maintenance of Certification competencies for Patient Care, Medical Knowledge, and Practice-Based Learning and Improvement.